

# Development Testing of the Gateway Integrated Bipropellant Refueling Subsystem

Adela D. Han<sup>1</sup>, Pooja S. Desai<sup>2</sup>, Brian S. Lusby<sup>3</sup>, Brandie L. Rhodes<sup>4</sup>,  
*NASA Johnson Space Center, Houston, Texas, USA*

Christopher D. Radke<sup>5</sup>  
*NASA Johnson Space Center, Houston, TX, 77058, USA*

The Lunar Gateway is a deep space orbiting outpost being developed by the National Aeronautics and Space Administration (NASA) in partnership with the European Space Agency (ESA) and other domestic and international partners. Because Gateway is a vital component of NASA's Artemis program supporting long-term human exploration of the moon, it is designed for on-orbit refueling to allow for a longer life performance. The reaction control system (RCS) bipropellant refueling system onboard the station will have the capability to transfer propellants, monomethyl hydrazine (MMH) and mixed oxides of nitrogen-3 (MON-3), under controlled conditions and will span across three modules: the European System Providing Refueling Infrastructure and Telecommunication Refueling Module (ESPRIT-RM or ERM), the Habitation and Logistics Outpost (HALO), and the Propulsion and Power Element (PPE). These propellant transfers are complex operations with known hazards, and one of the risk areas is exceeding the flight system's maximum design pressure (MDP) in priming and refueling pause/stop operations. In priming, liquid propellant is transferred from a pressurized source tank to evacuated transfer lines, which could result in excessive transient surge pressures and potentially damage hardware. In refueling pause/stop operations, fast-acting isolation valves (IV) are closed, which could lead to damaging water hammer. To mitigate these risks and develop the system, a collaborative NASA/ESA/Thales Alenia Space – United Kingdom (UK) test program was completed at Thales Alenia Space-UK on a simplified refueling breadboard representing ERM, HALO, and PPE bipropellant transfer systems. The objectives of the integrated breadboard testing were to (1) gather performance data to characterize and demonstrate critical refueling operations, (2) help inform flight designs, and (3) to validate numerical models that can be extended to predicting flight system performance. Integrated breadboard test data has shown the architected system performance is closing initial design assumptions. Further testing with propellant on a higher fidelity fluid simulator and analysis are planned.

## I. Nomenclature

$a$  = speed of sound in a fluid  
 $C_v$  = flow coefficient  
 $K$  = flow resistance K Factor  
 $\Delta P$  = pressure differential  
 $\Delta P_J$  = transient pressure change  
 $\rho$  = density  
 $v$  = velocity  
 $\Delta v$  = velocity change

---

1 Test Engineer (Jacobs Technology), Propulsion Systems Branch.

2 Test Director, Energy Systems Test Area.

3 Fluid Dynamics Analyst, Propulsion Systems Branch.

4 Senior Project Lead, Propulsion Systems Branch.

5 Gateway Chemical Propulsion System Manager, Propulsion Systems Branch.

## II. Introduction

Gateway will be an orbiting lunar outpost supporting the long-term human return to the surface of the Moon and providing a staging point for deep space exploration. A rendering of Gateway is shown in **Fig. 1**. The PPE can be seen on the far right connected to HALO, while the ERM is located on the northern radial port of HALO.

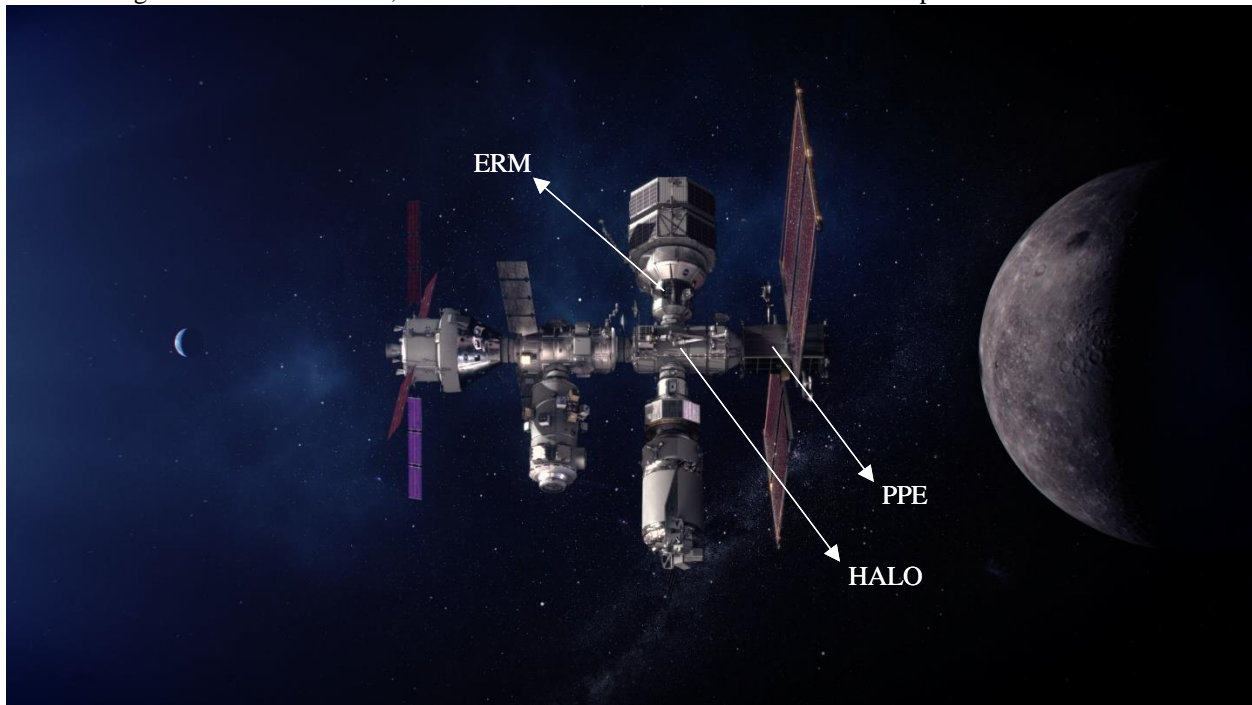


**Fig. 1: Rendering of Gateway, with elements from international partners (Credit: NASA/Alberto Bertolin).**

The first two modules of Gateway to be launched are PPE and HALO. Together these are referred to as the Co-manifested Vehicle (CMV). The PPE includes a bipropellant chemical propulsion system that will provide attitude control for Gateway. HALO will be the initial crew quarters for visiting astronauts and will have several docking ports for visiting vehicles and future modules. The ERM, provided by ESA, will provide the propellant refueling function to Gateway's RCS. MMH and nitrogen tetroxide (NTO) with three percent nitric oxide (NO), otherwise known as MON-3, will be transferred from ERM through HALO to PPE. A reduced schematic of the bipropellant refueling system is shown in **Fig. 2**.

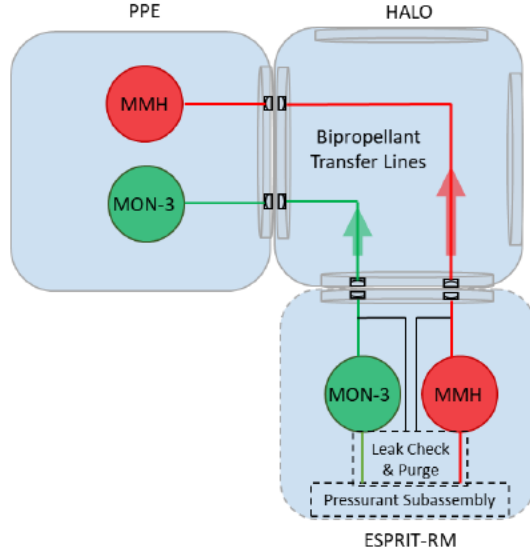


**Fig. 2: Reduced Schematic of the Bipropellant Transfer System**

On-orbit spacecraft refueling can generally be broken down into four phases: (1) mating, initialization, and leak checks, (2) propellant priming, (3) propellant transfer, (4) propellant venting and closeout activities. The integrated breadboard testing at Thales Alenia Space-UK primarily targeted activities (2) and (3) due to the higher likelihood of pressure transients that could exceed system planned operating pressures during these events.

### III. Integrated Breadboard System Description

Testing of the integrated breadboard was accomplished by combining two independently developed fluidic networks. The CMV breadboard was built as an early developmental test bed at NASA Johnson Space Center (JSC) and underwent an extensive test campaign prior to being shipped to Thales Alenia Space-UK for integration with the ERM breadboard (referred to as ERM-1) [2]. Each breadboard alone provided extensive insight into the independent systems, but together they provided holistic, integrated data to understand the fluid dynamics of on-orbit Gateway refueling, while saving cost and time by using representative commercial-off-the-shelf (COTS) components.

Two simulants were used in the place of bipropellants to allow development testing: water as a simulant for MMH and hydrofluoroether-7100 (HFE-7100) as a simulant for MON-3. Fluid density and speed of sound are the most desirable fluid properties to simulate for characterizing water hammer effects. From the Joukowski equation shown in Eq. (1), which is good for initial estimates of transient peak pressures, transient pressure change is dependent on the fluid density and speed of sound. The vapor pressure is another important parameter to simulate vapor front at the fluid head to characterize its effects on vacuum priming. Lastly, although the effect of viscosity is expected to be minor, it contributes to the fluid flow characterization. Water and HFE-7100 are common inert simulants for MMH and MON-3, respectively, due to their similarities in combination of density, speed of sound, vapor pressure, and viscosity. See **Table 1** for the fluid properties comparison.

$$\Delta P_J = -\rho a \Delta v \quad (1)$$

**Table 1: Fluid Properties Of MMH, Water, NTO, and HFE-7100 at ambient (14.7 psia, 77 F)**

	<b>MMH</b>	<b>Water</b>	<b>NTO</b>	<b>HFE-7100</b>
<b>Vapor Pressure (psia)</b>	0.957	0.46	17.375	3.902
$\rho$ , <b>Density (lb/ft3)</b>	54.3	62.2	89.5	94.4
$a$ , <b>Speed of Sound (ft/s)</b>	5079	4911	3205	1942
<b>Viscosity (cP)</b>	0.776	0.89	0.396	0.577

Water was the primary simulant used for most of the test cases due to its low cost, whereas only selected cases were used with the HFE-7100 engineering fluid. Testing with the second simulant provides the advantage of another reference point in terms of calibrating analyses, as well as giving a good idea of the flow performance in flight of the MON-3 propellant transfer.

A reduced schematic of the integrated breadboard system is shown in **Fig. 3**. Components that are not necessary to communicate primary results have been removed. In the schematic, fluid flows left to right, starting at the ERM tank. The system routes to a simplified section representing the rest of ERM and HALO before it tees into the PPE with one leg going to the PPE tank and the other to the PPE venting valve. Refueling is completed through a pressure-differential process, where the ERM tank is pressurized with helium at a higher pressure than the PPE tank, thus initiating and sustaining flow. The PPE vent valve (VV) is used to purge liquid out of the system after refueling transfer is complete.

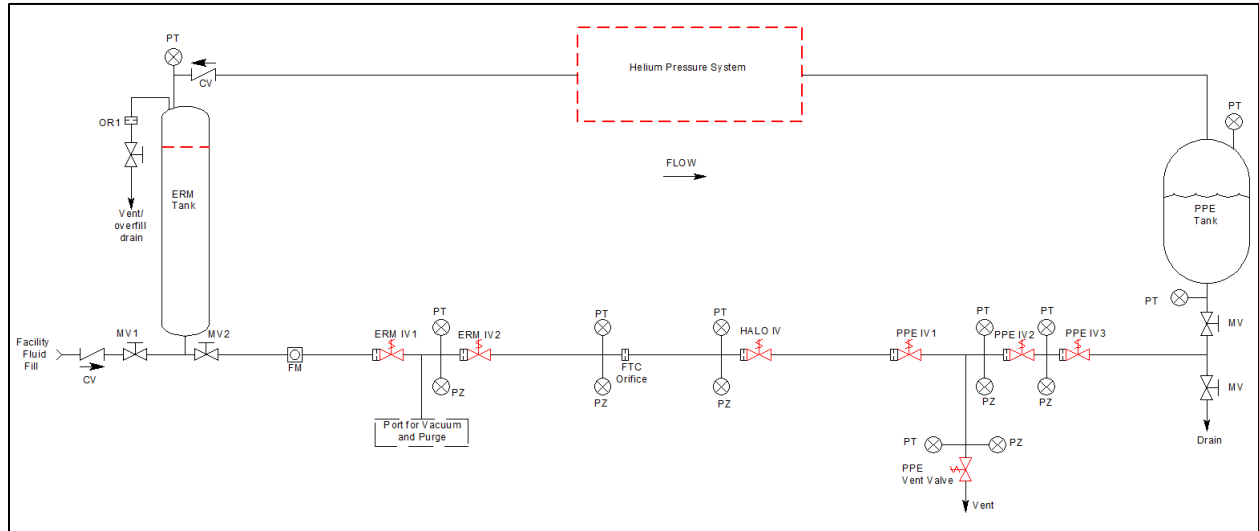


**Fig. 3: Simplified Breadboard Schematic**

The breadboard fluid system did not use any flight hardware, but representative COTS components were used. Subscale tanks were used to represent the ERM and PPE propellant tanks. Manual valves were used to fill the ERM tank with water, pressurize the tank with helium, and control flow to the vacuum and purge systems. Fast-acting solenoid valves were used to represent flight valves and emulate their response times as best as possible.

COTS filters with similar size and pressure drop characteristics as the flight components were used throughout the experimental apparatus at flight locations. The pressure drops for flight components that could not be fully represented in this developmental test were captured by using square-edge orifices. The tubing outer diameter used in each module was flight representative as well. Length of the tubing was flight representative to the greatest extent possible with the information provided. There were some lines that were reduced in length or not incorporated (such as PPE flight fill and drain lines) because these were not considered to have a major effect on the surge pressures in the priming and refueling pause/stop operations.

The system was also equipped with instrumentation sensors for measuring pressure, temperature, solenoid valve timing, and flow rate. The pressure and temperature sensors were calibrated prior to testing. The flow meter calibration was expired, however due to the time constraint, it was decided to be acceptable after verifying its readings with the calculated flow rates from the ERM tank scale. Critical peak pressure data was measured by a combination of piezoelectric sensors (PZs) and strain gauge pressure transducers (PTs) on the CMV breadboard. These were installed into manifolds at locations expected to experience the most significant water hammer events, particularly upstream of the solenoid valves. Kistler electroresistive pressure sensors were used on the ERM breadboard. The ranges of the pressure sensors were selected to capture expected and unexpected high transient pressures. The description of the pressure sensors used are shown in **Table 2**.

**Table 2: Integrated Breadboard Sensors Specification.**

Pressure Sensor Description	Vendor	Engineering Range (psia)	Resolution (psia)	Accuracy (FSO, psia)
CMV Strain Gauge Transducer	Taber Transducer	0-3000	0.18	$\pm 0.25\%$ , $\pm 7.5$
CMV Piezo Sensor	PCB	0-5000	0.31	$\pm 0.20\%$ , $\pm 10$
ERM Piezoresistive	Kistler	15-5076	0.16	$\pm 0.1\%$ , $\pm 5$

Valve electrical current data was measured to provide solenoid valve opening timing. The approximate opening times of the solenoid valves are shown in **Table 3**.

**Table 3: Integrated breadboard Solenoid Valves Opening Description**

Valve	Vendor	Opening Time* (ms)	Closing Time** (ms)
CMV Valve	Circle Seal	$80 \pm 3$	$19 \pm 8$
ERM Valve	Burkert	$15 \pm 3$	$65 \pm 15^{***}$

\*Opening time is time from command to when the poppet is open.

\*\* Closing time is time from command to when the poppet is closed.

\*\*\* ERM valve closing time was not measured and the number listed is from the manufacturer spec.

Data was recorded at 1 Hz and/or 10 kHz depending on the needs of the specific test. High speed data collection was limited to the highly dynamic fluid transient events due to the large file sizes. Control was provided by a LABVIEW graphical user interface (GUI) with a visual schematic with indicators for all instrumentation and on/off buttons for all solenoid valves. The GUI also featured warnings for max file size and solenoid valve overheating conditions.

Images of the integrated breadboard system are shown in **Fig. 4** to **Fig. 5**.



**Fig. 4: Integrated Breadboard System at Thales Alenia Space-UK Lab**

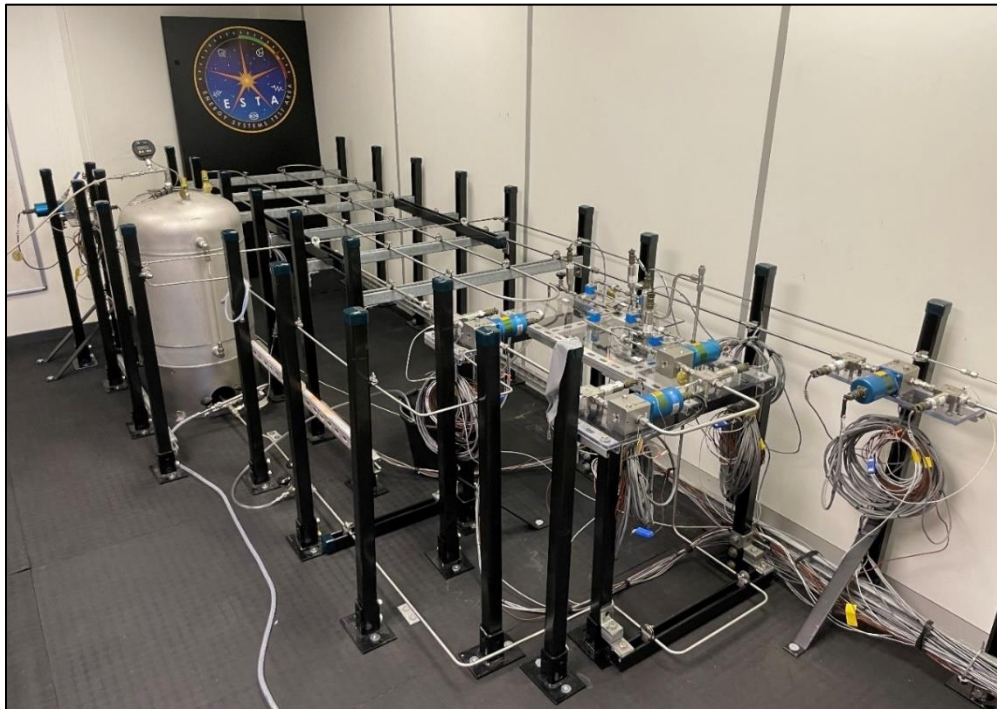


**Fig. 5: NASA CMV Breadboard at Thales Alenia Space-UK Lab**

#### **IV. Integrated Breadboard Test Description**

The integrated test program was performed between May 23, 2022 and September 14, 2022. In this program, four types of operations were performed with the breadboard at Thales Alenia Space-UK: (1) priming, (2) flow characterization, (3) refueling pause, and (4) refueling transfer. Each type of operation is described in more detail below.

##### **A. Priming**

The primary objective of the priming tests was to evaluate the surge pressures at critical locations in the system at varying ERM tank pressure with both water and HFE-7100. The initial vacuum condition is an extremely sensitive parameter that affects vacuum priming transient pressures. Cautious steps were taken to simulate flight like vacuum as much as possible to prepare for the priming test. A vacuum pump was connected to multiple locations on the system and was run for extended time to dry out any trapped residual liquid from previous operations and bring down the pressure. Once the vacuum gage reading stabilized, the system was isolated from the vacuum pump and the pressure was observed for a minimum of 5 minutes to confirm there was no significant reverse leakage and no presence of residual liquid vaporizing and raising vacuum pressure. In addition, as the initial operation to each priming stage, the system was once again isolated from the vacuum pump for 10 seconds, and the vacuum level was verified to be stable. The 10 second observation time was decided from the maximum duration required and limited from vacuum pump isolation to opening of the priming valve.

In these tests, fast-acting isolation valves separated the higher pressure fluid supply from downstream tubing runs pre-set at a vacuum. When the isolation valves were opened, the downstream lines were primed, and the pressure transients were recorded. The water priming tests were performed at 3 different ERM tank pressure ranges which will be referred to as low, medium, and high pressure due to the publication sensitivity of this data. The HFE-7100 priming tests were only performed at low and medium pressure. For most of the test cases, 3 stage priming was implemented: in stage 0, from the ERM IV1 to the ERM IV2, then in stage 1, from the ERM IV2 to the HALO IV, and lastly in stage 2, from the HALO IV to the PPE IV2 and PPE vent valve. This is demonstrated in **Fig. 6** below. An additional

mid pressure water test case combining stage 1 and stage 2 was performed from the ERM IV2 to the PPE IV2 and PPE vent valve, as illustrated in **Fig. 7**. As a second additional medium pressure water test case, a 3 stage priming to helium pressurized lines instead of vacuum lines was performed.

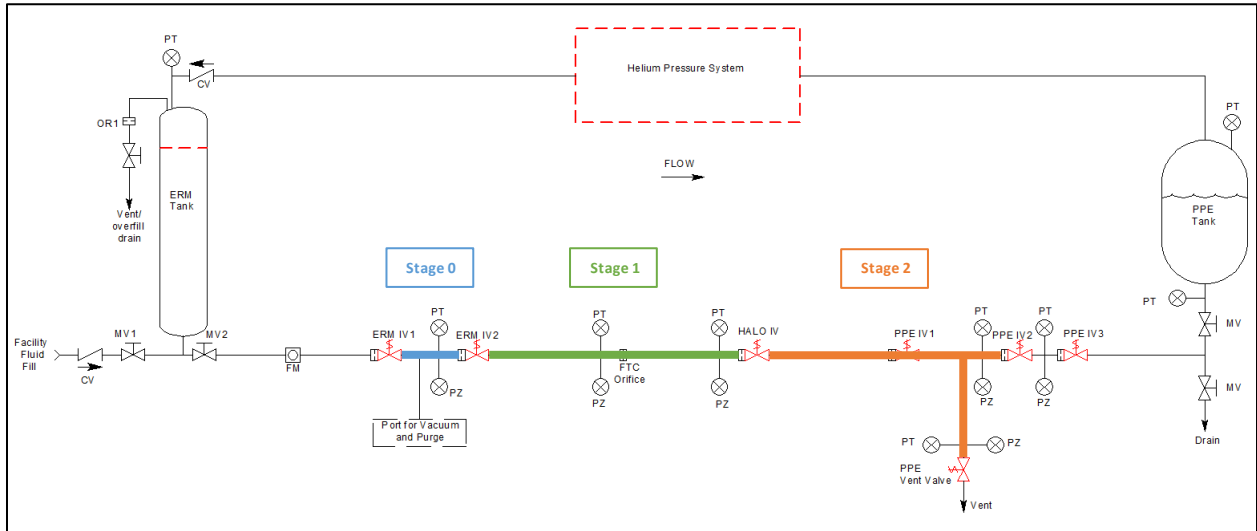


**Fig. 6: 3 Stage Priming Volumes**

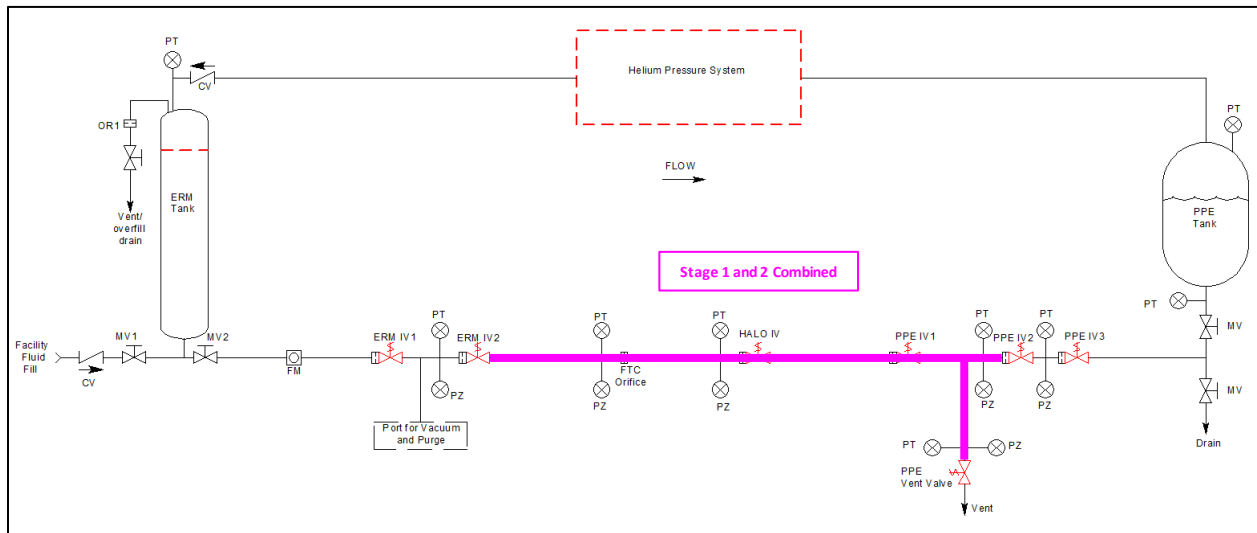


**Fig. 7: Combined Stage 1 and Stage 2 Priming**

## B. Flow Characterization

The main purpose of the flow characterization tests was to characterize the pressure drop of each component or section at various steady state flow rates. This was achieved by adjusting ERM tank pressures and having the PPE tank opened to ambient pressure. The tests were run with water and HFE-7100.

### **C. Refueling Pause**

The primary objective of the refueling pause tests was to evaluate the surge pressures at critical locations after a valve is closed to simulate a pause or stop in refueling. Prior to this test, the fluid lines were vacuum primed to avoid trapped gas, which is a sensitive factor for pressure transients. Also, the transient peak pressure is highly dependent on the flow rate. In this test, the target flow rate was achieved by adjusting the ERM tank pressure to set the correct pressure differential from the ERM tank to the PPE tank. After steady flow was established and verified with the flow meter reading, either the ERM IV2, HALO, or PPE IV2 was closed.

Initially, the refueling pause operation pressure was not considered as a sensitive parameter for pressure transients, therefore the refueling tests were done at various pressures referred to low and medium, which are the same pressure range referred to in priming test cases. Later, after test data evaluation, the tank pressure was also discovered to be a sensitive parameter for pressure transients. This observation is described in more detail in section **V. C. (2)**. Tests were performed with both water and HFE-7100.

### **D. Refueling Transfer**

The purpose of the refueling transfer tests was to demonstrate fluid transfer between ERM and PPE via the blowdown method. These tests were done with water only.

## **V. Test Data and Discussion**

This section presents a summary of the data collected during the integrated test program and key data takeaways. At locations where two different pressure sensors were installed, the peak pressure from the pressure sensor with the higher reading was recorded.

### **A. Priming**

Priming test cases were performed with many variables, including simulant, priming pressure, priming volume, and initial line pressure condition (vacuum/helium pressurized) to evaluate their impacts on transient peak pressures. **Fig. 8** shows a representative plot of the transient pressure event from a priming sequence. The delta transient peak pressure is calculated by subtracting the settling pressure from the maximum transient peak pressure. The settling pressure is determined by the Taber strain gauge transducer since the piezoelectric sensor is only suited for dynamic situations. The piezoelectric sensor's signal decays over time due to its impedance (as seen by the blue curve in Fig. 8). **Table 4** and **Table 5** summarize the delta transient peak pressure data collected from water and HFE-7100 priming test cases.

Each test case was performed two times to verify repeatability except for the Stage 1 priming to a helium pressurized line case. The repeated test run for this case was found invalid after the completion of the test program. The numbers presented in **Table 4** and **Table 5** are values from each priming test case.

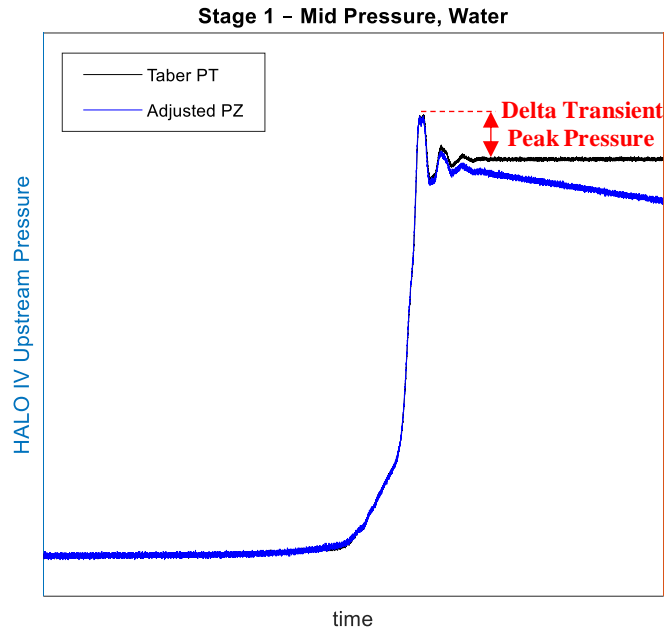


**Fig. 8: HALO IV Upstream Transient Pressure during Stage 1 Mid Pressure Water Priming**

**Table 4: Water Priming Data**

Priming Stage	ERM Tank Pressure	Approximate Priming Volume (in <sup>3</sup> )	Initial Line Pressure	Peak Pressure Location	Delta Peak Pressure (psid)
Stage 0	Low	3 to 4	<0.1 torr	Upstream ERM IV 2	7, 7
Stage 0	Mid		<0.1 torr		24, 26
Stage 0	Mid		9 psia		2, 3
Stage 0	High		<0.1 torr		69, 70
Stage 1	Low	21	<0.1 torr	Upstream HALO IV	3, 4
Stage 1	Mid		<0.1 torr		12, 15
Stage 1	Mid		4 psia		0
Stage 1	High		<0.1 torr		64, 68
Stage 2	Low	48	<0.1 torr	Upstream PPE Vent Valve	1, 2
Stage 2	Mid		<0.1 torr		12, 16
Stage 2	Mid		7 psia		1, 1
Stage 2	High		<0.1 torr		31, 34
Stage 1 & 2 Combined	Mid	67	<0.1 torr	Upstream FTC Orifice, Upstream PPE Vent Valve	9, 9

**Table 5: HFE 7100 Priming Data**

Priming Stage	ERM Tank Pressure	Approximate Priming Volume (in <sup>3</sup> )	Initial Line Pressure	Peak Pressure Location	Delta Peak Pressure (psid)
Stage 0	Low	3 to 4	<0.1 torr	Upstream ERM IV 2	1, 3
Stage 0	Mid		<0.1 torr		11, 11
Stage 1	Low	21	<0.1 torr	Upstream HALO IV	0, 1
Stage 1	Mid		<0.1 torr		3, 5
Stage 2	Low	48	<0.1 torr	Upstream PPE Vent Valve	0, 0
Stage 2	Mid		<0.1 torr		2, 3

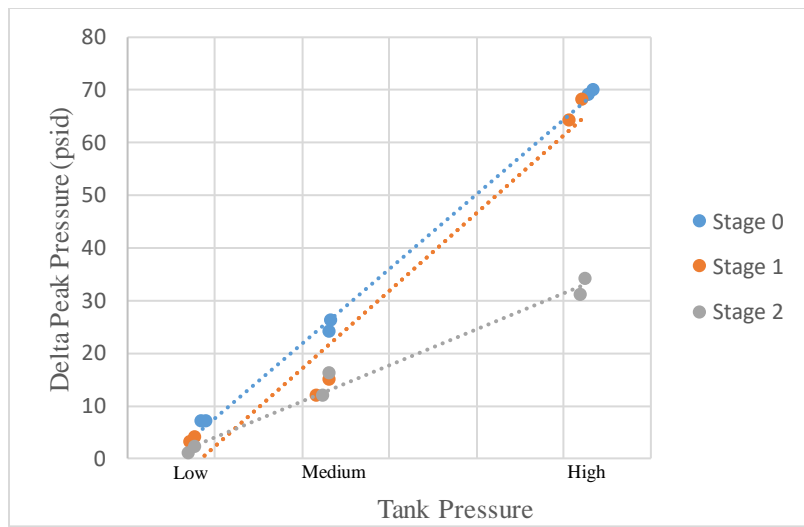


**Fig. 9: Delta Peak Pressure vs. Tank Pressure for Different Stages – Water**

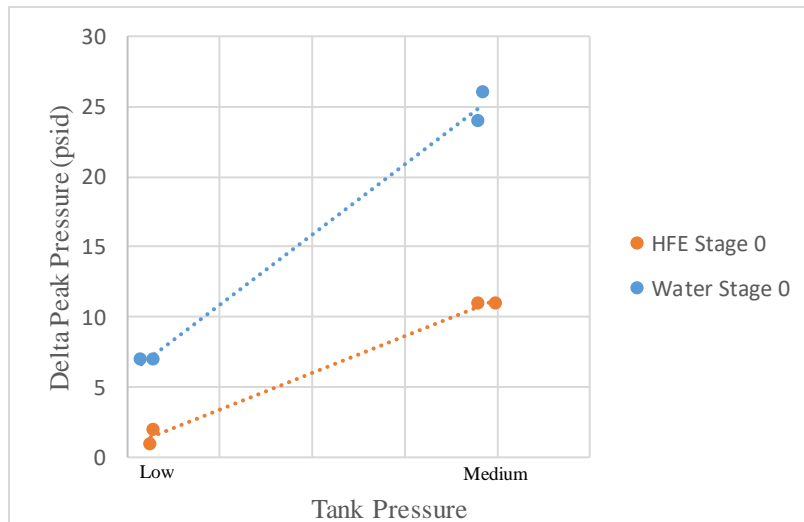


**Fig. 10: Delta Peak Pressure Comparison of HFE and Water – Stage 0 Priming**

Key Observations from Priming Tests:

- (1) Location of Peak Pressures: Generally, the highest transient peak pressure occurred right upstream of the dead end of the priming volume. If there is any component with low flow coefficient ( $C_v$ ) in the priming volume, it is possible that the upstream of the component will have higher peak pressure than the dead end of the priming volume. **Table 6** below is a delta peak pressure data set example from the stage 2 high pressure water priming case. Delta peak pressures at the PPE vent valve is the highest and decreases as it goes upstream of the priming volume dead end.

**Table 6: Example Stage 2 – Mid Pressure Priming Delta Peak Pressures**

Location	ERM IV2 Upstream	FTC Orifice Upstream	PPE IV2 Upstream	PPE Vent Valve Upstream
Delta Peak Pressure (psid)	12	17	25	31

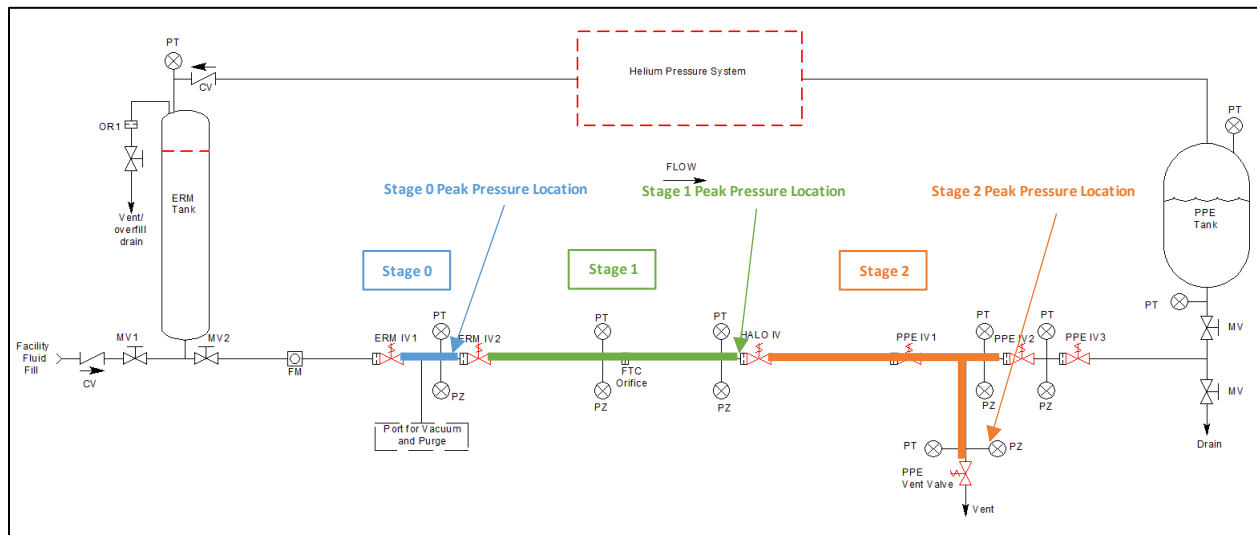


**Fig 11: Priming Peak Pressure Locations of 3-Stage priming**

- (2) Tank Pressure: The tank pressure and the delta peak priming transient pressure appear to roughly have a linear relationship as shown in **Fig. 9**.
- (3) Fluid Property Impact: Delta peak pressures from HFE-7100 priming were observed to be slightly lower compared to water. **Fig. 10** shows the comparison between water and HFE-7100 priming cases at low and medium pressures for Stage 0. This can be explained by examining the Joukowski Equation, shown in Eq. (1), in combination with a form of the Bernoulli equation, shown in Eq. (2). The Joukowski equation shows that the transient overpressure is a function of the fluid's density, speed of sound, and velocity just before the liquid column impacts the dead end. The Bernoulli Equation shows that the velocity of the fluid is a function of its density and the pressure differential forcing the liquid to fill the lines. It can be shown that by combining these two equations and substituting fluid properties from Table 1, the ratio of expected surge pressure of water to HFE-7100 is approximately 2 to 1. Higher vapor pressure of HFE-7100 is another factor that possibly contributed to HFE-7100 having a lower priming delta peak pressure compared to water. It is expected that a larger vapor front is created due to the higher vapor pressure.

$$\Delta P_J = -\rho a \Delta v \quad (1)$$

$$\Delta P = K\rho \frac{v^2}{2} \quad (2)$$

- (4) Initial Line Pressure: Priming to low pressure He pressurized lines significantly reduced the pressure transients to almost negligible.
- (5) Distance from Priming Source: The magnitude of the delta peak pressures was generally lower as the priming end gets further downstream from the priming source. This is due to the sum of flow restrictions of the upstream priming volume being larger, resulting in a lower flow rate and a lower transient delta peak pressure.
- (6) Stage 1 and Stage 2 Combined: It was observed that the stage 1 and stage 2 combined priming transient delta peak pressures did not show a significant difference compared to the stage 1 or stage 2.

## B. Flow Characterization

The data collected from flow characterization test was used to build the analysis model and was not technically evaluated.

## C. Refueling Pause

Refueling pause test cases were performed with a few variables, including simulant, ERM tank pressure, the closing valve, and flow rate to evaluate their impacts on transient peak pressures. Transient peak pressures were observed upstream and downstream of the closing valve. **Fig. 12** shows a representative plot of the transient pressure event upstream of an isolation valve right after the valve was closed to pause the flow. **Fig. 13** shows a representative plot of the transient pressure event downstream of the valve. The delta transient peak pressure was calculated in the same way as was done for priming. Each test case was performed two times to verify repeatability. The numbers presented in **Table 7** show the delta transient peak pressure data collected from each refueling pause case.

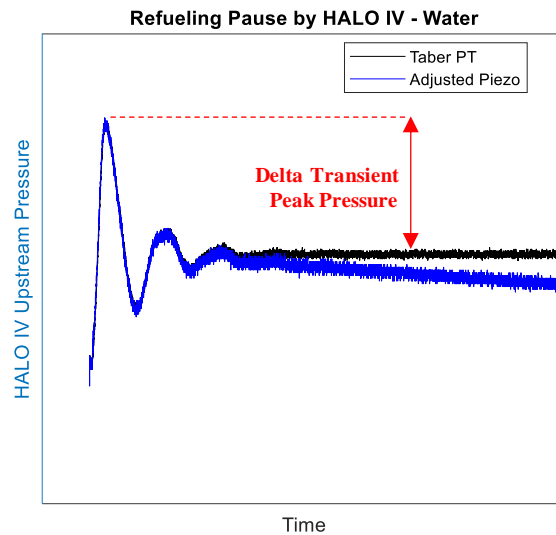


Fig. 12: HALO IV Upstream Transient Pressure during Water Refueling Pause

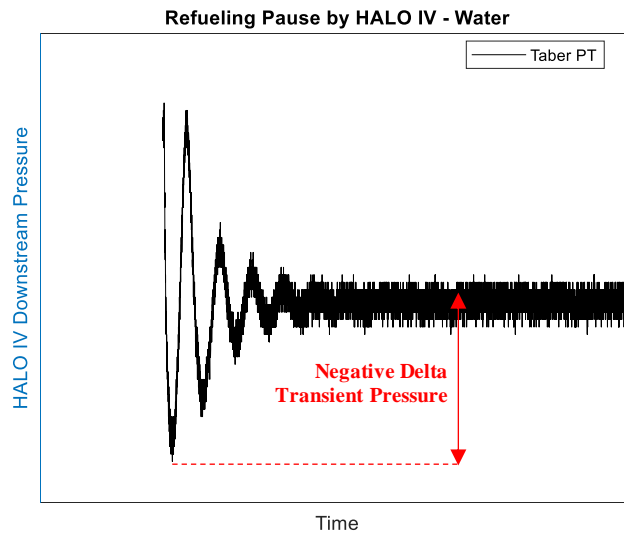


Fig. 13: HALO IV Downstream Transient Pressure during Water Refueling Pause

**Table 7: Refueling Pause Data**

Closing Valve	Case Description	ERM Tank Pressure	Actual to Target Flow Rate Ratio	Peak Pressure Location	Upstream Delta Peak Pressure (psid)	Downstream Negative Delta Pressure (psid)
ERM IV2	Water Run 1	Low	1.11	ERM IV2 Upstream	18	10
ERM IV2	Water Run 2	Low	1.11	ERM IV2 Upstream	14	9
ERM IV2	HFE-7100 Run 1	Mid	1.00	ERM IV2 Upstream	30	34
ERM IV2	HFE-7100 Run 2	High	1.14	ERM IV2 Upstream	32	39
HALO IV	Water Run 1	Low	1.11	HALO IV Upstream	16	4
HALO IV	Water Run 2	Low	1.14	HALO IV Upstream	25	7
HALO IV	HFE-7100 Run 1	Mid	0.99	HALO IV Upstream	34	18
HALO IV	HFE-7100 Run 2	High	1.00	HALO IV Upstream	33	18
PPE IV2	Water Run 1	Low	1.11	PPE IV2 Upstream	4	3
PPE IV2	Water Run 2	Low	1.17	PPE IV2 Upstream	7	5
PPE IV2	HFE-7100 Run 1	Mid	1.00	PPE IV2 Upstream	27	30
PPE IV2	HFE-7100 Run 2	High	1.05	PPE IV2 Upstream	28	28

**Key Observations From Refueling Pause Tests:**

- (1) Location of Peak Pressure: The highest transient delta peak pressures were observed just upstream of the closing valve.
- (2) Tank Pressure: Initially, the refueling pause operation pressure was not considered as a sensitive parameter for pressure transients, so the refueling tests were done at various pressures referred to as low and medium, which are the same pressure range referred in priming test cases. Later, after test data evaluation, the tank pressure was discovered to be a sensitive parameter for pressure transients. The transient delta peak pressures were observed to be higher when the operating pressures were higher at comparable flow rates. This is due to the larger effect of entrained gas at low pressure. As the operating pressure increases, the effect of entrained gas is reduced as shown in **Fig. 14**. **Fig. 14** shows the pressure dependency of the transient pressure change with 0, 0.01, 0.1, and 1 percent entrained gas in water derived from the Joukowsky and Wood's equations.

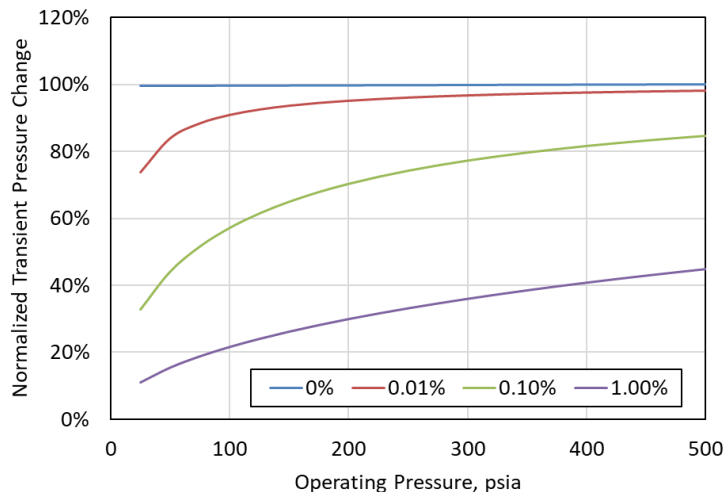


**Fig. 14: Pressure Dependency of Transient Pressure Change of Water with Various Entrained Gas Percentage (Derived from the Joukowsky and Wood’s Equations).**

- (3) Fluid Property Impact: Unfortunately, because water and HFE-7100 refueling pause data was collected at different tank pressures, fluid impact on delta peak pressure cannot be evaluated with the collected data. However, the expected effect of fluid property to the delta peak pressure is the same as it is described in the priming data summary section, V. A. (3). With the Joukowsky Equation, shown in Eq. (1), in combination with a form of the Bernoulli equation, shown in Eq. (2), the ratio of expected transient delta peak pressure of water to HFE-7100 is approximately 2 to 1 at comparable operation pressure and flow rate.
- (4) Location of Closing Valve: The refueling pause transient delta peak pressures were very dependent on the location of the closing valve. In this test set up, the HALO IV closure produced higher delta peak pressures compared to PPE IV2 closure. ERM IV2 closure also produced higher delta peak pressures compared to PPE IV2, but this is not a direct comparison due to different valves used for ERM IV2 and PPE IV2. In general, it is observed that the transient pressure will vary depending on the system design around the closing valve and valve closing time.
- (5) Downstream Transient Pressure: The initial transient response on the downstream side of a valve closing is pressure dropping followed by resonance. The transient pressure drop is more aggressive when the upstream delta peak pressure is higher. The lowest transient pressure drop needs to be evaluated to stay above propellant vapor pressure. The vaporization and collapse of the vapor pocket will create violent heat transfer. At Gateway RCS refueling operation pressures, the minimum transient pressure expected from the breadboard test data is higher than the propellant vapor pressure.
- (6) Flow Rate: The flowrate was kept consistent throughout each test case as best as possible within the pre-determined acceptable range. However, even within the pre-determined acceptable range, the delta peak pressure results from the test cases show that it is highly sensitive to the flow rate.

#### D. Refueling Transfer

The data collected from refueling transfer test was used to develop concept of operation and was not technically evaluated.

### VI. Model Validation with Test Data

A numerical model of the breadboard system was developed using Thermal Desktop Version 6.1 with FloCAD [3]. Thermal Desktop is a powerful general-purpose thermal and fluid modeling software that is widely used throughout the aerospace industry. The Thermal Desktop add-on module, FloCAD, provides the capability to graphically model fluid flow circuits typically encountered in spacecraft fluid transfer systems. Thermal Desktop was chosen for this modeling application due to its flat-front two-phase flow modeling capability, which is ideal for modeling the filling of liquid into a tubing system that initially contains a gas at low pressure or is evacuated.

A similar numerical model was previously developed for the CMV breadboard testing at JSC, and a detailed description of the modeling methodology and validation is described in Ref. [2]. The CMV breadboard model was used as the starting point for the integrated breadboard model with modifications to include the additional ERM

breadboard tubing and components. One significant difference for integrated breadboard testing is in addition to water, HFE-7100 was used as a second propellant simulant. During the initial model correlation effort, it was determined that the nonvolatile formulation of HFE-7100 was insufficient to adequately capture the pressure rise rate during priming surge pressure events. As a result, a simplified two-phase fluid formulation was developed based on fluid property data provided by the manufacturer.

One of the key performance parameters for the priming test runs is the transient peak pressure. For each priming stage, the transient pressure just upstream of the dead end was measured. A comparison summary of the stage zero priming delta peak pressures just upstream of ERM IV2 is shown below in **Fig. 14**. The model results correlate very well with the test data and follow the same trend. The variability in model results at a given tank pressure is attributed to slightly different initial vacuum conditions. No test runs were performed at the high tank pressure for HFE-7100.

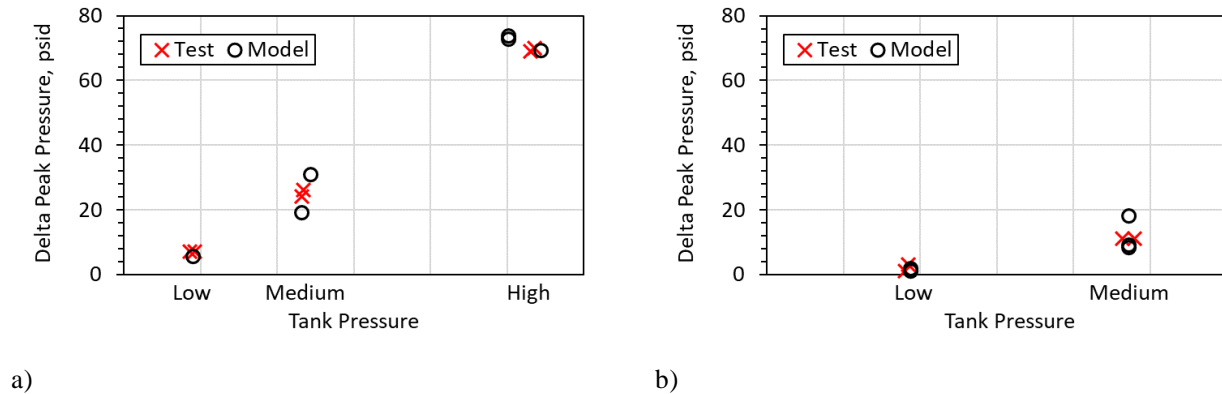


**Fig. 14: Stage zero priming delta peak pressures for a) water and b) HFE-7100 upstream of ERM IV2.**

A comparison summary for the stage one priming delta peak pressures just upstream of the HALO IV is shown below in **Fig. 15**. Again, the model results correlate very well with the test data for the low and medium tank pressure cases. The transient peak pressures for the high tank pressure cases tend to be underpredicted by the model, but the difference is close to within the accuracy of the sensors.

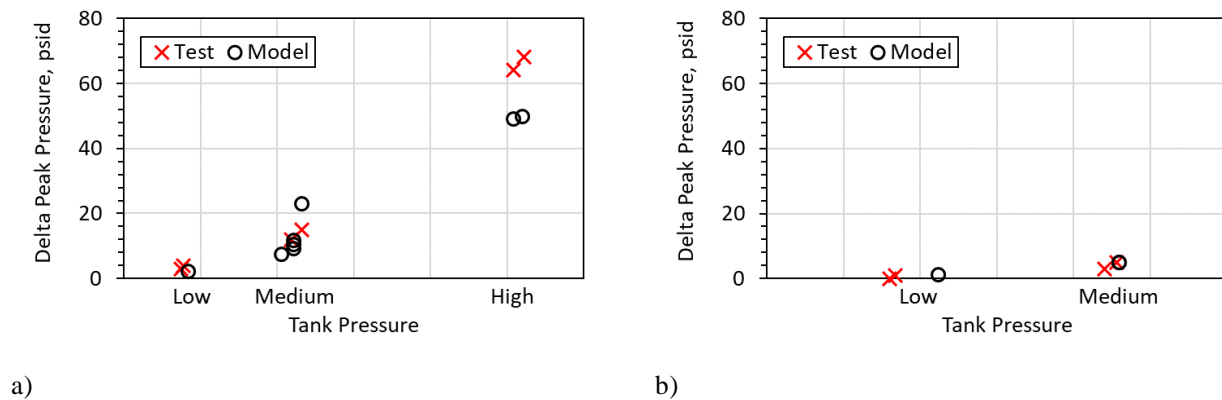


**Fig. 15: Stage one priming delta peak pressures for a) water and b) HFE-7100 upstream of the HALO IV.**

A comparison summary for the stage two priming delta peak pressures just upstream of the PPE VV is shown below in **Fig. 16**. A numerical instability was identified during stage two priming model runs with HFE-7100, which caused the model to crash after multiple days of run time. Therefore, no comparisons could be made with the HFE-7100 test data. However, this was not considered to be an issue since the test data showed that surge pressures were

minimal. The results trend in a similar way compared to stage one with the transient peak pressures at high tank pressures being underpredicted by the model. The difference is within the accuracy of the piezoelectric sensors.

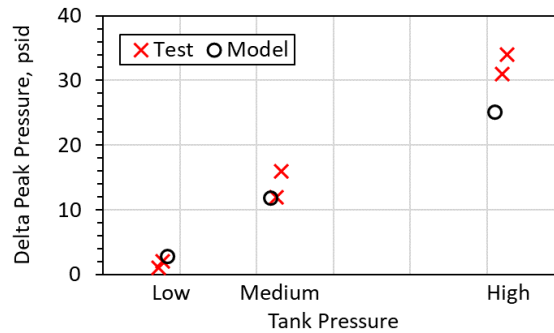


**Fig 16: Stage two priming delta peak pressures for water upstream of the PPE VV.**

## VII. Conclusion

Refueling technology contributes to the extension of spacecraft life. However, refueling architecture and operations need to be developed carefully to prevent failure and mitigate hazards for successful operation. Surge pressure during refueling operations was a pre-defined risk for the system, and the integrated breadboard test served as a tool to define and control this risk. The test data also significantly contributed to initial development of the Gateway flight RCS, including flow control design, refueling requirements, and concept of operations.

Fluid dynamics of the refueling operation are very system dependent, and it is critical to build and test a system that is highly flight representative. The breadboard system was designed with the best information available at the time. Also, there are other known risks for refueling that were not verified in the integrated breadboard test program to consider, such as temperature and pressure rise in the liquid locked section during refueling pauses or some failure mode, un-combusted propellant freezing during line venting, and leak development during propellant transfer. Therefore, further testing with propellant on a higher fidelity fluid simulator and analysis are planned for accurate and full insight of expected fluid behavior during flight operation.

## Acknowledgments

The authors would like to extend their thanks to the many people that have supported the work presented here: Bill Holton (Electrical Technician), Clinton McLain (Mechanical Technician), Hunter Zambrano (Mechanical Technician), Matthew Green (Software Engineer), Humberto Hernandez (System Management), Rollin Christianson (Senior Engineer), Samuel Jones (Senior Engineer), Michael Reddington (Test Manager), and Brian Nufer at NASA-KSC for review of the test data. Additionally, thanks go to NASA's European partners in support of the breadboard testing: Sebastian Hill (TAS-UK), Andrew Hughes (TAS-UK), Olivier Zagoni (TAS-France), and Alexandra Bulit (ESA).

## References

- [1] Hill, S., Hughes, A., Wellons, G., Hoyland, L., Rhodes, B., Han, A., Lusby, B., Desai, P., Radke, C., Zagoni, O., and Leonardi, M., "Joint Development Testing of the Integrated Gateway-ESPRIT Bipropellant Refuelling System," SP2022 Paper 393, May 2022.
- [2] Lusby, B., Rhodes, B., Han, A., Desai, P., Green, M., and Radke, C., "Validation of Transient Spacecraft Refueling Model with Gateway Breadboard Test Data," AIAA SciTech, January 2023.
- [3] Thermal Desktop, Software Package, Ver. 6.1, Cullimore and Ring Technologies, Inc., Boulder, CO, 2019.